NeuroImage 191 (2019) 549–559

Contents lists available at ScienceDirect

NeuroImage

journal homepage: www.elsevier.com/locate/neuroimage

Decoding the status of working memory representations in preparation of visual selection

Ingmar E.J. de Vries *, Joram van Driel, Christian N.L. Olivers

Department of Experimental and Applied Psychology, Faculty of Behavioural and Movement Sciences, Vrije Universiteit Amsterdam, Van der Boechorststraat 1, 1081BT, Amsterdam, Netherlands

ARTICLE INFO

Keywords:
EEG decoding
Cognitive control
Task preparation
Neural oscillations
Visual attention
Visual search

ABSTRACT

Daily life is filled with sequences of multiple tasks, each with their own relevant perceptual input. Working memory needs to dissociate representations that drive attention towards currently relevant information from prospective representations that are needed for future tasks, but that until then should be prevented from guiding attention. Yet, little is known about how the brain initiates and controls such sequential prioritization of selection. In the current study we recorded EEG while subjects remembered a color as the target template for one of two sequential search tasks, thus making it either currently relevant (when it was the target for the first search) or prospectively relevant (when it was the target for the second search) prior to the task sequence. Using time-frequency specific linear classifiers, we were able to predict the priority status (current versus prospective) of the memory representation from multivariate patterns of delta (2–4 Hz) and non-lateralized alpha power (8–14 Hz) during both delay periods. The delta band was only transiently involved when initializing the priority status at the start of the first delay, or when switching priority during the second delay, which we interpret as reflecting the momentary top-down control over prioritization. In contrast, alpha power decoding was based on a more stable pattern of activity that generalized across time both within and between delay periods, which we interpret as reflecting a difference in the prioritized memory representations themselves. Taken together, we reveal the involvement of a complex, distributed and dynamic spatiotemporal landscape of frequency-specific oscillatory activity in controlling prioritization of information within working memory.

1. Introduction

Attending to what is relevant while ignoring what is not, is of utter-most importance for the successful navigation through an ever-changing visual environment. Such goal-directed behavior is thought to be mediated by template representations of task-relevant information that help guide attention to the matching visual input (Desimone and Duncan, 1995; Duncan and Humphreys, 1989), and which are assumed to be activated in visual working memory (VWM; Bundesen, 1990; Wolfe, 1994). Furthermore, as we typically perform sequences of multiple tasks, the relevance of information rapidly changes according to our moment-by-moment perceptual goals (Nobre and Van Ede, 2018). As such, working memory not only serves as storage for currently relevant representations that are needed for the imminent, upcoming task, but it also maintains prospectively relevant representations needed for future tasks. To prevent interference, prospective representations are shielded from biasing attention while observers are performing (Carlisle and Woodman, 2011; Peters et al., 2009), or preparing for (Olmos-Solis et al., 2018, 2017; van Loon et al., 2017), the current task. Consequently, theories distinguish different states in VWM, assuming currently relevant representations that are allowed to interact with sensory input, and prospectively relevant representations that are stored in a latent, de-prioritized and potentially silent state for later use (LaRocque et al., 2016, 2014; 2013; Lewis-Peacock et al., 2012; Myers et al., 2017b; Oberauer and Hein, 2012; Olivers et al., 2011; Stokes, 2015; van Loon et al., 2018; Wolff et al., 2017; Yu and Postle, 2018).

While these studies provide converging evidence for a dissociation between the actual functional and neural representations of differently prioritized memory items, it remains largely unknown which mechanism *controls* this prioritization. Here we approached this question by recording EEG while subjects performed two sequential visual search tasks, as illustrated in Fig. 1a. Prior to the task sequence, a single target color was presented, which was either relevant for the first, current search task, or for the second, prospective search task. No target template

* Corresponding author.
E-mail address: i.e.j.de.vries@vu.nl (I.E.J. de Vries).

https://doi.org/10.1016/j.neuroimage.2019.02.069
Received 12 November 2018; Received in revised form 27 January 2019; Accepted 27 February 2019
Available online 3 March 2019

was required for the other search task in the sequence. To assess which spectrotemporal landscape is associated with controlling current and prospective states of task preparation, we performed multivariate pattern analyses (MVPA) of time-frequency decomposed EEG data during the delay periods both prior to and between the searches. Based on initial evidence from one of our earlier studies (de Vries et al., 2018), we hypothesized that frontal delta oscillations play a key role in controlling relative priorities of task-related representations. In that study, participants memorized two colors instead of one, after which they looked for each of these colors in two sequential visual search tasks. One memory item was always presented left or right from fixation, while the other was presented on the vertical meridian, above or below fixation. We manipulated the priority of the laterally presented memory item (i.e. it was needed for either the imminent or the prospective search task), enabling us to directly relate hemisphere-specific EEG dynamics to a memory item with a specific status. First, we found stronger suppression of alpha power contralateral to the prioritized memory item (see also de Vries et al., 2017), which switched in sign along with cognitively switching priority from one working memory to the next in between search tasks. Second, we found evidence of a cross-frequency coupling mechanism supporting the top-down control of priority switches: the lateralized posterior alpha suppression effects were predicted by both phase and amplitude of frontal delta oscillations. This finding converges with other evidence pointing to a key role of frontal low-frequency (delta-to-theta) oscillations in the top-down control of VWM (Johnson et al., 2017; Onton et al., 2005; Sauseng et al., 2010), and task switching (Sauseng et al., 2006).

However, while our earlier findings indicate that frontal delta reflects the control of *switching* between two subsequent tasks, we did not observe evidence for similar top-down control signals during the first delay period, when the tasks need to be set up, and thus the different priority states of the memories involved need to be *initialized*. This raises the question whether implementing different states of currently relevant versus prospectively relevant memories is fundamentally different from switching between such states. Alternatively, our previous design and analyses may not have been optimal for detecting such implementation mechanisms, for several reasons. First, in de Vries et al. (2018), both a current *and* a prospective item were to be remembered during the first delay, thus potentially obscuring any dissociation between states – especially in global, non-lateralized signals (though see de Vries et al., 2017). Second, the start of the first delay period coincided with memory encoding. This could be especially problematic in combination with the fact that we used univariate analyses on selected electrodes. That is, memory encoding may have obscured subtle differences between state-related signals that distribute across multiple electrodes. Indeed, recent work has indicated that the different processes involved in VWM control may well be supported by distributed brain regions (Christophel et al., 2017), and thus the spatial pattern of neural activity underlying the top-down control of prioritization in VWM may be more complex and widespread than can be captured by traditional univariate EEG measures.

Recently, multivariate pattern analysis (MVPA) of EEG data has been advocated for the study of higher order brain states, as it can pick up on such complex scalp patterns of neural activity (e.g. Cichy and Pantazis, 2017; LaRocque et al., 2014; Mayr and Kikumoto, 2018; Stokes et al., 2015). Here we applied MVPA to see if it can uncover the specific anticipatory control states involved in preparing working memory for either an imminent or a prospective visual task, and if so, whether this preparation is specific to a certain frequency. To this end, we designed the task sequence such that it consisted of two consecutive search tasks, but only a single item had to be remembered. We then manipulated the relevance of the memory item for either the upcoming or the prospective search task. For the remaining search task no memory was required. Thus, and importantly, an item always had to be stored in memory, but what changed was whether it was required for the first or second task, and thus whether observers were preparing for a working-memory driven task. Differentially prioritizing a working memory representation depending on the upcoming task demands presumably reconfigures its representational state in service of those task demands, to optimize perception-action mapping (Myers et al., 2017b). Here, we predicted specifically that the delta frequency range would provide dissociable signals both during initialization of the priority status, as well as when switching priority between tasks. Furthermore, we investigated how the pattern of oscillatory activity involved in setting the priority relates to the pattern involved in switching priority in between search tasks, by employing generalization across time analyses (King and Dehaene, 2014). In addition to comparing global state-related signals, we presented memory items lateralized to the left or right from fixation, in an attempt to replicate the hemisphere-specific modulations of alpha power in response to the priority status of the memory item that we found earlier (de Vries et al., 2018). Last, in order to compare our MVPA results with traditional univariate approaches we also explored whether we could find a univariate non-lateralized control signal in the broad time-frequency landscape across the scalp.

2. Material and methods

All raw data and analysis scripts used to derive at the here presented results are available on OSF at osf.io/p4qfz.

2.1. Subjects

Twenty-eight healthy human subjects with normal or corrected-to-normal vision participated for course credit or monetary compensation. In total, five subjects were removed due to bad performance (one subject, 67% accuracy), too many trials with horizontal eye movements during the memory display (one subject, 27% of trials), too many noisy trials (one subject, 24% of trials), or a combination of the above (two subjects with only ~50% of trials left after data cleaning). This left 23 subjects (12 female, 25 ± 3 years old) for all analyses. The procedures used were conducted in accordance with the Declaration of Helsinki and were positively reviewed by the faculty's Scientific and Ethical Review Board. Written informed consent was obtained.

2.2. Task design

Fig. 1a illustrates the trial procedure. Each trial started with a fixation cross (1400–1800 ms, randomly jittered), consecutively followed by a memory display (400 ms), the first delay period (1400 ms), the first search display (until response), the second delay period (1800 ms), and the second search display (until response). The memory display consisted of four colored circles surrounding fixation. Subjects memorized the one color that had either a dashed or dotted outline, while the other three colors had a full outline and could be ignored. The type of outline (dashed or dotted) indicated whether the color was relevant for the first or second search task, with its meaning counterbalanced across subjects. In the Current condition (Fig. 1a, upper row), the memorized color was the target on the first search task (referred to as "template-based search"). In this condition, the second search task did not require subjects to remember a color. Instead, the second search task involved displays in which the participant had to find any two neighboring identical colors (referred to as "duplicate-color search"). Importantly, this search task did not require a color to be stored as search template in visual working memory. In the Prospective condition (Fig. 1a, lower row) the order of the two types of search tasks was reversed. Thus, subjects first searched for any pair of identical colors (duplicate-color search), and then searched for the memorized color (template-based search). Note that one color had to be remembered regardless of task order, but the conditions differed in whether this color was relevant for the first (Current) or second (Prospective) task. Each of the six circles in the search display contained an arrow, with equal amounts of randomly divided left- and right-pointing arrows. Upon finding the target color, subjects responded to the direction of the arrowhead plotted inside the target by clicking on a

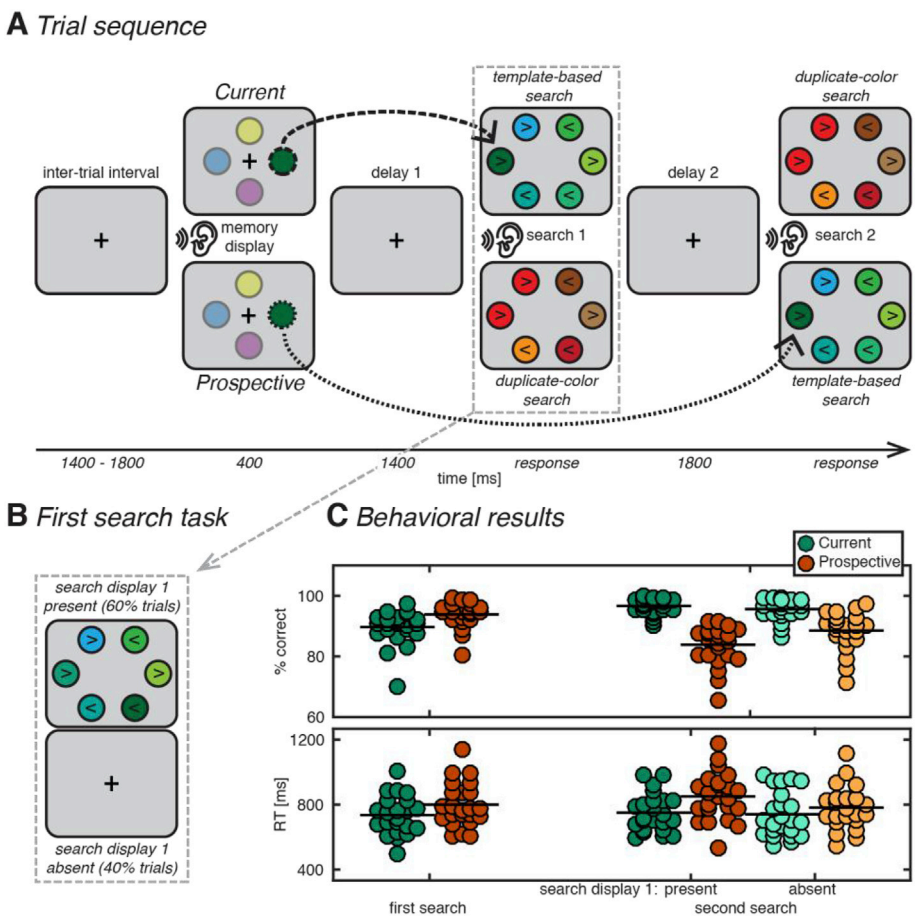

Fig. 1. Task design. (a) Trial sequence. Subjects were given one color to remember (From a display of four), after which they performed two consecutive search tasks. The memory item was always presented left or right from fixation, and it was either needed for the first search task in the "Current" condition (top row; here dashed outline), or for the second search task in the "Prospective" condition (bottom row; here dotted outline). No color had to be remembered for the remaining search task as here subjects searched for any color that appeared twice (i.e. *duplicate-color search*). Stimulus display onsets were accompanied by a beep. For illustrative purposes, object sizes and colors differ from the real experiment and the irrelevant colors in the memory displays are drawn with 50% opacity. (b) To prevent the perception of and response to the first search display from interfering with the reactivation of the prospective search template, we omitted the first search display in a random 40% of trials; here the screen remained blank (with fixation cross) and the second delay period started. The combination of the sound and the absence of the first search display cued subjects they should switch from first to second search. (c) Behavioral results. Dots represent single subject behavioral results (percentage correct and trial-averaged correct RT in upper and lower panel, respectively). Horizontal line segments represent the group mean. Results for the second search task are separated into trials where the first search was present (left, darker shades) or absent (right; brighter shades).

left or right hand button (placed on each armrest) corresponding to the direction of the arrow. In the duplicate-color search display the two identically colored target circles had an arrow pointing in the same direction. Subjects received a 50 ms 660 Hz auditory cue at the onset of each display (memory, search 1 and search 2). Subjects were instructed to focus on the central fixation cross during the inter-trial interval, the memory display and both delay periods. The memory item was always presented either left or right from fixation, enabling us to directly relate lateralized EEG patterns to the memory item on that trial. Note that while only two laterally presented circles were necessary in the current design, we also presented two circles on the vertical midline in order to keep the design close to our previous design (de Vries et al., 2018, 2017).

In a random subset of 40% of the trials, the first search display was omitted, and the screen remained blank (with fixation cross) as the second delay period started (Fig. 1b). However, the auditory cue that normally indicated the onset of the first search display was still presented. Crucially, the sound now served as a warning cue, informing subjects that they could abandon preparing for the first search task, and instead switch to preparing for the second search task. The reason for presenting the auditory cue at the onset of all three displays in 100% of trials was to ensure that subjects would maximally associate the sound with display onset, such that a sound without such an onset would be a clear signal to endogenously switch task goals. In all our EEG analyses involving the second delay period, we focused on these 40% of trials in which the first search display was omitted, and which were thus free from any perceptual and response-related signals from the first search task perturbing the second delay period. Note that in none of our analyses we directly compared trials with and without first search task, as this would potentially be biased by stimulus-induced activity. Subjects performed one practice block followed by 20 experimental blocks, each consisting of the same randomly ordered composition of 30 trials: 15 per condition (Current and Prospective), and for each condition 9 with, and 6 without first search task.

2.3. Stimuli

Stimuli were created using Opensesame version 2.9.0 (Mathôt et al., 2012, RRID:SCR_002849), a Python based experiment builder, and presented on a 22-inch screen (Samsung Syncmaster 2233, 1680 × 1050 pixels at 120 Hz) viewed from 75 cm. The background was grey (81 Cd/m^2). The black fixation cross had line lengths of 0.6°. The memory colors were presented 1.5° from fixation and had a radius of 0.6° with a black outline of 0.09°. The six colored circles in the visual search display were presented 4° from fixation, equidistantly from each other. Stimulus colors were created in DKL color space (Derrington et al., 1984) with constant luminance (i.e. 0) and contrast (i.e. 1), but varying in hue (from 12 to 324° in steps of 24°, skipping 108 and 156 because they were subjectively too similar to neighboring colors). This created a color space of twelve discrete colors, evenly spaced on a circle (41.2 ± 4 Cd/m^2). First, the memory color was randomly chosen, after which the three to be ignored colors were randomly chosen, each at least 2 steps away from the memory color on the color circle (to prevent too strong similarity). In the template-based search display the memorized color returned as the target, together with five other colors randomly chosen from the eight colors surrounding the memorized color on the color circle. Thus distractors were chosen to be relatively similar, to prevent verbalization and force the use of visual working memory. For the duplicate-color search display all five colors, including the duplicate color itself, were randomly chosen, and at least 2 steps away from the memorized color that served as the target for the other (template-based) search task on that trial. This was done to ensure that the memorized color on that trial was *not* present as a distractor in the duplicate-color search display. The auditory cue was

generated by OpenSesame's built-in synthesizer, consisted of a 50 ms 660 Hz sine wave and was presented by a HK195 speaker.

2.4. Data recording and preprocessing

EEG data were acquired at 512 Hz using a 64-electrode cap (BioSemi, Amsterdam, The Netherlands; ActiveTwo system, 10–20 placement; www.biosemi.com), and from both earlobes (reference). Vertical and horizontal EOG were recorded from electrodes located 2 cm above and below the right eye, and from electrodes 1 cm lateral to the external canthi, respectively. Offline analyses were performed in Matlab (2014a, The Mathworks, RRID:SCR_001622).

Unless indicated otherwise, preprocessing was done using built-in functions and their default parameter settings as implemented in the EEGLAB toolbox (Delorme and Makeig, 2004, RRID:SCR_007292). First, data were re-referenced to the average of both earlobes and high-pass filtered at 0.1 Hz using EEGLAB's pop_filtnew function. Continuous EEG was epoched from −2.5–8 s surrounding memory display onset. Epochs were baseline-normalized using the whole epoch as baseline to improve independent component analysis (ICA (Groppe et al., 2009)). Data were visually inspected and one (n = 4), two (n = 7), three (n = 2) or four (n = 1) malfunctioning electrodes were temporarily removed. We used an adapted version of the automatic trial-rejection procedure as implemented in the Fieldtrip toolbox (Oostenveld et al., 2011, RRID:SCR_004849) on the 110–140 Hz band-pass filtered data to specifically detect muscle artifacts, and allowed for individual z-score cut-offs. This resulted in a cut-off of 18 ± 4.3, and a rejection of 4.7% (min-max across subjects: 0.3–14.5%) of all trials. Next, we performed ICA on clean trials and electrodes only. On average, we removed 1.8 ± 0.5 ICA components capturing eye movements or blinks (confirmed by the VEOG signal), or other artifacts that were clearly not brain-driven, after which we interpolated malfunctioning electrodes identified earlier using EEGLAB's eeg_interp.m function (i.e. spherical spline interpolation). Last, we rejected trials in which subjects made horizontal eye movements during lateralized memory encoding using the pop_artstep function from ERPLAB (Lopez-Calderon and Luck, 2014, RRID:SCR_009574), applied to the 1 Hz high-pass filtered HEOG signal, with a 400 ms window sliding with 10 ms steps, from −50 to 900 ms surrounding memory display onset, and with individual thresholds of 17 ± 3.2. This resulted in a rejection of 8% (min-max across subjects: 0.5–19%) of all trials.

After data cleaning based on the EEG signals, we also rejected error trials (14%, min-max across subjects: 7–24%), and trials with a response faster than 300 ms, slower than 5000 ms, or a response of 3 standard deviations above or below the condition- and search task specific mean (2.3%, min-max across subjects 0.8–3.3%). After all trial rejection procedures (noise, HEOG, error and RT), 73% of all trials remained for the main analyses (min-max across subjects: 57–87%). As a last preprocessing step we applied a spatial high-pass filter by means of the surface Laplacian (Perrin et al., 1989), thereby accentuating local effects while filtering out distant effects due to volume conduction, thus sharpening the EEG topography (Cohen, 2014; Kayser and Tenke, 2015). We estimated the surface Laplacian using a 10^{th}-order Legendre polynomial and a lambda of 10^{-5}. Importantly, while all trials were used for analyses of the first (memory cue-locked) delay period, only trials in which the first search task was omitted (40%) were used for analyses of the second (auditory switch cue-locked) delay period, as these trials did not suffer from interference caused by the first search task.

2.5. Time-frequency decomposition

We applied Morlet wavelet convolution to decompose the EEG time series into time-frequency representations using custom-written Matlab scripts, for frequencies ranging from 1 to 40 Hz in 25 logarithmically spaced steps. Specifically, a Gaussian ($e^{-t^2/2s^2}$, where s is the width of the Gaussian) was multiplied with 25 sine waves ($e^{i2\pi ft}$ where i is the complex operator, f is frequency, and t is time) to create complex Morlet wavelets. The width was set as $s = \delta/(2\pi f)$, where δ represents the number of cycles of each wavelet, logarithmically spaced between 3 and 12 to have a good trade-off between temporal and frequency precision. Frequency-domain convolution was applied, i.e. multiplication of the EEG data with the Morlet wavelets after applying the Fast Fourier Transform (FFT) to each, followed by a conversion of the resulting signal back to the time domain using the inverse FFT. The squared magnitude of these complex signals was taken at each time point and each frequency to acquire power, i.e. $[\text{real}(Z_t)^2 + \text{imag}(Z_t)^2]$. Power was further down-sampled to 64 Hz to reduce computation time. For univariate time series analysis, single-trial raw power was averaged over trials per condition, after which decibel normalization was applied per frequency and per channel [dB $\text{Power}_{tf} = 10*\log10(\text{Power}_{tf}/\text{Baseline Power}_f)$], with as baseline the condition-average power 500 to 200 ms priori to memory display-onset.

2.6. Multivariate pattern analysis

The main analysis involved a backward decoding classification algorithm (linear discriminant analysis or LDA) with all 64 channels as features and the Current and Prospective condition labels as classes, on time-frequency decomposed power. The goal of this analysis was to test whether a classifier could learn from differential topographical patterns of power modulations during the delay period of each single trial, to dissociate between an item being memorized for either a current or for a prospective search task. For this MVPA analysis we used the Amsterdam Decoding and Modeling toolbox (ADAM; Fahrenfort et al., 2018), an open source, script-based toolbox in Matlab for backward decoding and forward encoding modeling of EEG/MEG data (we replaced the standard time-frequency decomposition algorithm in that toolbox with our custom written time-frequency decomposition). Training and testing was done on the same data using a 10-fold cross-validation procedure: first, trials were randomized in order, and divided into 10 equal-sized folds; next, a leave-one-out procedure was used on the 10 folds, such that the classifier was trained on 9 folds and tested on the remaining fold. This procedure was repeated 10 times until each fold was used once for testing. Classifier performance was then averaged over folds. We applied within-class balancing using under-sampling for the location at which the memory item was presented, such that the number of left-cue and right-cue trials was the same within each class. This procedure ensured that the training of the classifier was not biased by memory location. Additionally, we applied between-class balancing using over-sampling to ensure that during training the classifier would not develop a bias for the over-represented class. Note that as the design was balanced in terms of trial counts for memory location (left versus right) and memory status (Current versus Prospective), within- and between-class balancing was only necessary to account for small imbalances due to trial rejection procedures used for data cleaning. As a measure of classifier performance, we used the Area Under the Curve (AUC), with the curve being the receiver operating curve of the cumulative probabilities that the classifier assigns to instances as coming from the same class (true positives) against the cumulative probabilities that the classifier assigns to instances that come from the other class (false positives). AUC takes into account the degree of confidence (distance from the decision boundary) that the classifier has about class membership of individual instances, rather than averaging across binary decisions about class membership of individual instances (as happens when computing standard accuracy). As such the AUC is considered a sensitive, nonparametric and criterion-free measure of classification (Hand and Till, 2001). An AUC value of 0.5 means chance level classification performance. In our initial decoding analysis, this decoding classification procedure was executed for every time-frequency point, thus yielding the evolution of classifier performance over time and frequency.

Next, to investigate the topographical distribution of neural activity underlying significant classification, we computed topographical maps by multiplying classifier weights of all electrodes with the covariance

matrix of the data across electrodes (Haufe et al., 2014). This procedure generates activation patterns that return the mass-univariate difference between the compared conditions, but which unlike classifier weights, can be interpreted as neural sources. Last, we performed a generalization across time (GAT) analysis (King and Dehaene, 2014). In this analysis, the classifier is not only tested on the same time point at which it was trained, but tested across all other time points as well. This yields a "temporal generalization matrix" of time-by-time classification accuracy, which informs about whether a pattern of neural activity underlying classification performance is stable, or whether it dynamically evolves over time.

2.7. Statistics

2.7.1. Behavioral analyses

Behavior was analyzed with Bayesian paired-samples t-tests on both RT and accuracy data using JASP (Version 0.7.1.12, RRID:SCR_015823), a GUI-based software package for performing Bayesian statistics (Marsman and Wagenmakers, 2017). Bayesian hypothesis testing can evaluate whether the data provide evidence in favor of either the alternative or the null hypothesis, with the Bayes Factor (BF) being an interpretable numerical expression of the strength of this evidence (Rouder et al., 2009; Wagenmakers et al., 2017).

2.7.2. EEG

On the univariate trial-averaged time-frequency results, we applied two lines of group-level statistics. First, we investigated whether lateralized posterior alpha power would show stronger suppression for current versus prospective target representations (de Vries et al., 2018, 2017). For this analysis, we a priori selected the frequency range of 8–14 Hz, and electrodes O1/2, PO3/4 and PO7/8, based on previous results from our lab (de Vries et al., 2018; van Driel et al., 2017), and subtracted ipsi-from contralateral electrodes. Second, we performed an exploratory, mass-univariate statistical analysis on non-lateralized (i.e. irrespective of the memory cue location) power including all time-frequency-electrode points, to search for a cluster in which univariate power would be able to dissociate between target representations. Additionally, to increase statistical sensitivity we constrained this mass-univariate test to two a priori selected spatio-spectral ROIs, namely posterior alpha power (frequency range and electrodes as above), and frontal delta power (2–6 Hz in AFz/AF3; see de Vries et al., 2018), and performed the statistical test again for each of these time series. We used permutation testing with cluster-based correction for multiple comparisons, which takes into account the inherent auto-correlation between nearby time-, frequency-, electrode-pairs (Maris and Oostenveld, 2007). We set the threshold for significance at $p < 0.05$, performed 2000 iterations, and used the test statistic (i.e. *t*-values) summed over all significant points belonging to the same cluster to define the respective cluster size. Thus, only significant clusters larger than what can be expected by chance, survived this procedure. For any cluster-based permutation test involving all electrodes, we used Fieldtrip's ft_timelockstatistics.m function with the method parameter set to 'montecarlo' (Maris and Oostenveld, 2007; Oostenveld et al., 2011). We used the ft_prepare_neighbours.m function with the method parameter set to 'template' to define which electrodes are neighbours, and set the minimum number of neighboring significant electrodes to define whether electrodes were part of the same cluster to 1. We constrained all statistical tests to 200 ms surrounding the delay periods, i.e. −200 to 2000 ms relative to onset of the memory display or relative to the auditory switch cue for the first and second delay period, respectively.

In our univariate analysis we tested condition differences in power against baseline. Multivariate classification results were tested at the group level for AUC deviations from chance (i.e. 0.5). While testing against chance-level is common practice for information-based measures (Christophel et al., 2018; Cichy et al., 2014; Rose et al., 2016; Wolff et al., 2017), caution is warranted in making statistical inferences. Specifically, because 'true' population-level AUC values cannot fall below 0.5, while observed values in the tested sample can (due to estimation noise), this results in fixed-rather than random-effects inference (Allefeld et al., 2016). Consequently, one cannot draw population-level inferences, but is restricted to the sample that was tested, and the null-hypothesis being tested then becomes the hypothesis that in the population there is not a single person with above-chance classification. In other words, under these conditions one can only infer that there are some subjects in the sample with above-chance decoding. While further development of methods for the statistical inference of information-based measures is paramount, this goes beyond the scope of the current study. In the meantime, to support our findings, we also report the prevalence of the effects in our sample, i.e. the number of subjects with an AUC > 0.5 (see Supplementary Material).

3. Results and discussion

3.1. Behavior

On average, subjects performed well (first search task: 92% ± 5; second search task [first search task present]: 90% ± 4; second search task [first search task absent]: 92% ± 5; Fig. 1c, upper panel). Accuracy was better on the duplicate-color search task compared to the template-based search task, both on the first ($BF = 6.3*10^4$), and on the second search task ($BF = 1.2*10^8$). This is not surprising, given that for this search task all relevant information was present in the display itself, whereas the template-based search task had to rely on memory. Accuracy on the template-based search task was overall lower when this task was presented second compared to when it was presented first ($BF = 4.6*10^5$). However, if the template-based search task was cued to be the second search task, but the first search task was omitted, memory performance on that template-based search task was comparable to trials in which it was cued to be the first search task ($BF = 0.96$). Reaction times showed a similar pattern (Fig. 1c, lower panel). Specifically, subjects responded slower on the template-based search task if it was the second compared to the first search task ($BF = 1.4*10^6$), but to a much lesser extent if the first search task was omitted ($BF = 3.2$). Importantly, this pattern indicates that subjects remembered the search target equally well regardless of whether it was cued to be used first or second, and that memory performance on the second search task decreased due to interference from the first search task. Thus, in accordance with previous findings (de Vries et al., 2018; Myers et al., 2017a; Rerko and Oberauer, 2013; Van Moorselaar et al., 2015; Wang et al., 2018), manipulating the priority status of the memory item did not affect memory quality *per se*.

3.2. Multivariate frequency-specific power is sensitive to the momentary task-relevance of a single VWM representation

We first applied the MVPA approach to test our hypothesis that frequency-specific oscillatory activity would dissociate between preparing memorized targets that are currently versus prospectively relevant. Specifically, at each time point of both delay periods, we trained a linear discriminant classifier to dissociate between the Current and Prospective conditions using frequency-specific power at all 64 electrodes as features. Interestingly, this multivariate analysis revealed status-sensitive information in the spectral profiles of the EEG. Specifically, in line with our hypothesis, we observed significant decoding in the delta band in both the first delay period (1.8–4 Hz by 250–900 ms relative to memory display onset, $p < 0.05$ cluster-corrected; Fig. 2a, left panel), as well as in the second delay period (1.8–3.4 Hz by 700–1200 ms relative to the switch cue, $p < 0.05$ cluster-corrected; Fig. 2a, right panel). Importantly, the here observed effects of above-chance decoding were not driven by a few subjects, but were present in the majority (i.e. between 17–21 out of 23 subjects; see Fig. S1). We note that we replicated this effect emerging during the first delay period by re-analyzing the first delay period of two similar conditions from one of our previous studies (de Vries et al., 2017),

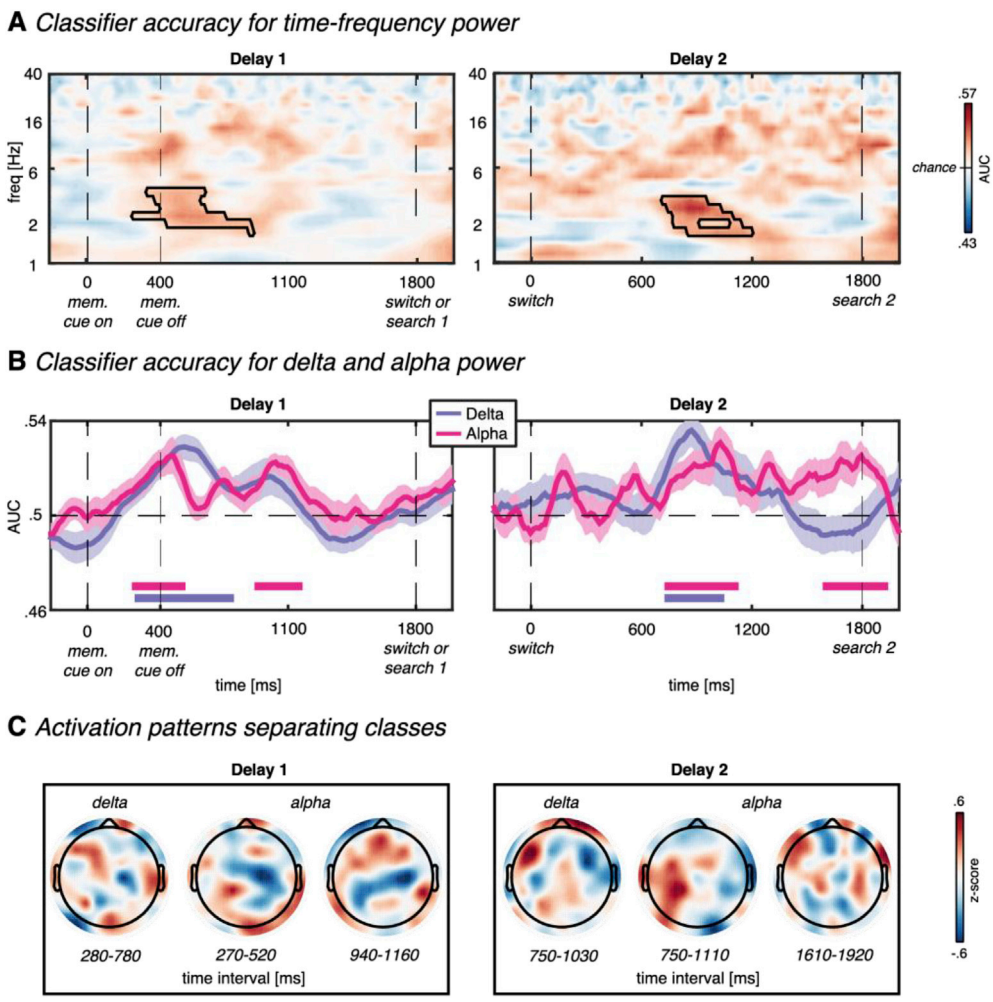

Fig. 2. MVPA decoding of priority status. (a) Time-frequency maps of classifier accuracy (AUC). The left and right columns illustrate delay 1 (including all trials in decoding analysis) and delay 2 (including only trials where first search task was omitted, i.e. 40% of all trials), respectively. Black outlines indicate significant classification after cluster correction at $p < 0.05$. (b) Classifier accuracy plotted over time for delta (2–4 Hz; pink) and alpha (8–14 Hz; purple) bands. Thick lines and shaded areas denote subject mean and SEM, respectively. The thick horizontal bars indicate significant classification after cluster correction at $p < 0.05$. (c) Class-separability maps (Haufe et al., 2014) averaged over time windows of significant decoding (see b), and z-scored across channels.

see Supplementary Material). These results support a role for low-frequency oscillations in the executive control involved in working memory operations in general (Helfrich and Knight, 2016; Onton et al., 2005; Sauseng et al., 2010). We also previously found frontal delta-band oscillatory power to interact with lateralized posterior alpha-band power when switching the task-relevant priority from one memory item to the next (de Vries et al., 2018). Here, we demonstrate that long-range topographical patterns of delta oscillations are specifically involved in preparing for a working memory-driven visual search task, both during initialization of such a task, and when switching from a non memory-driven task to such a memory-driven task.

Given that, on the basis of our previous studies (de Vries et al., 2018, 2017; van Driel et al., 2017), we also had specific a priori hypotheses about the alpha frequency band, we next tested for above chance classifier performance for alpha (8–14 Hz) power specifically (Fig. 2b, pink line). Again, this multivariate approach showed an effect of memory status on long-range alpha-band patterns. Specifically, we observed significant alpha power decoding both during working memory encoding (270–520 ms), and in the middle of the first delay period (940–1160 ms), as well as during the second delay period (750–1110 ms), and at the end of the second delay period in anticipation of the second search task (1610–1920 ms). Again, above-chance decoding was present in the majority of subjects (Fig. S1). This suggests that alpha oscillations support prioritization while preparing a visual working memory representation for an upcoming perceptual task even when there is no direct retinotopic competition between multiple stored memory items (such visual competition between current and prospective items was present in our previous study de Vries et al., 2018). The topographical patterns of the forward-transformed classifier weights in the time windows of significant decoding (Fig. 2c), were of high spatial frequency, without clear clusters of electrodes exhibiting the same univariate difference between the Current and Prospective conditions. This further supports the involvement of oscillatory activity but within a complex spatial pattern, rather than bound to a specific (retinotopic) region. In addition, we speculate that the alpha power decoding effect during the early interval of the second delay period reflects prioritizing the prospective versus dropping the current memory representation, whereas alpha power decoding during the late interval of the second delay period reflects preparing for a template-based versus a duplicate-color search task. In contrast to delta power decoding, we did not observe above-chance alpha power decoding in our re-analysis of the first delay period from our previous dataset, presumably caused by subtle differences in experimental design (see Supplementary Material for a discussion). Finally, to test whether the observed effects were specific to oscillatory power-envelope fluctuations, we performed the equivalent analyses on broadband time-domain EEG activity (Fig. S2). This analysis resulted in significant decoding only while the search displays were on the screen, which likely reflects that this type of classifier picked up on general task-related differences between the template-based and duplicate-color search tasks themselves, rather than prioritization processes within working memory.

Last, we tested whether the spatial pattern of oscillatory activity underlying significant classification performance was stable, or whether it dynamically changed over time, using a time-by-time generalization approach (King and Dehaene, 2014). Delta power decoding was relatively short-lived and only increased in accuracy on the diagonal (i.e. where training and testing are done on the same time points), resulting in

small clusters of significant time-by-time points that did not survive cluster correction for multiple comparisons (Fig. 3a and Fig. S3b). Indeed, delta power decoding was significant when only testing on the diagonal (Fig. 2a and b, and Fig. S3a). Thus the data are indicative of not only a spatially diverse, but also a highly dynamic pattern of delta power separating current from prospective states. In contrast, alpha power decoding was not only present on the diagonal, as it also generalized to other time points (Fig. 3b). This means that the spatial pattern of alpha power that separated current from prospective states was stable during large parts of the delay periods. Note that this does not mean that alpha power decoding was sustained throughout the delay period, as can also be seen from the gaps in above-chance decoding (Figs. 2b and 3b). Rather, whenever there was above-chance decoding, the spatial pattern underlying this generalized to other time points within that delay period. Furthermore, whereas delta power decoding was only significant in one interval, alpha power decoding was significant in two intervals spread out over each delay period. Based on these findings, we speculate that delta power may be only momentarily involved in a top-down manner when initializing the priority status (first delay), or when re-initializing it (second delay), whereas alpha power may reflect the state of prioritization itself. Interestingly, we did not observe above chance cross-delay generalization. That is, the pattern dissociating priority states during the first delay period did not generalize to the second delay period, indicating that implementing the first state differed considerably from switching to the second state. In fact, there was evidence for a complete reversal of the pattern (Fig. 3b, cluster of significant negative decoding).

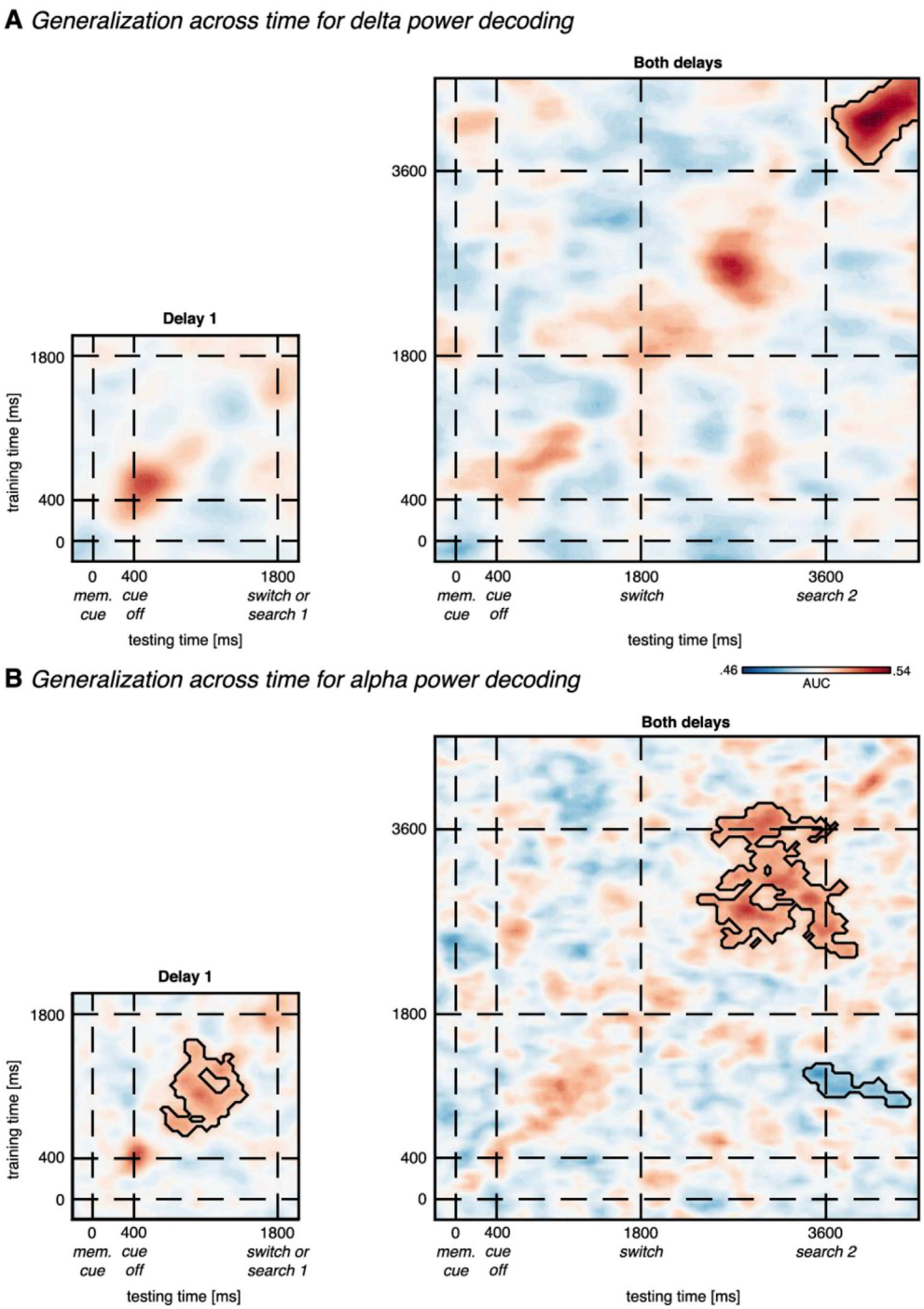

Fig. 3. Temporal generalization of classifier performance. (a) GAT matrix of delta (2–4 Hz) power decoding. Time points on which classifiers were trained/tested are plotted along the vertical/horizontal axis. The left map shows delay 1 (including all trials in decoding analysis); the right map shows the whole trial (including only trials where first search task was omitted, i.e. 40% of all trials). (b) Same as (a), but now for alpha (8–14 Hz) power. Black outlines indicate significant classification after cluster correction at $p < 0.05$.

Specifically, when training the classifier on the neural pattern separating priority states during the first delay period, and subsequently testing the classifier on the second search task, the classifier selected the wrong class more often than expected by chance ($p < 0.05$ cluster-corrected). In other words, the pattern that differentiated between the priority states was in fact similar during both these intervals, but as the priority state of the memory item reversed after the first search task, so did the neural pattern. Interestingly, recent fMRI findings also indicate that the neural pattern underlying significant decoding is inversed between priority states, i.e. training and testing on different priority states of the same memory representation resulted in below-chance decoding (van Loon et al., 2018; Yu and Postle, 2018).

It is important to note that in our analyses we did not decode the content of the memory representations *per se* (i.e. the color), but rather their relative *relevance* with respect to the behavioral task at hand. As such, the here observed significant decoding could be interpreted as reflecting the higher cognitive brain state of preparing working memory representations for either imminent or prospective visual search. While ample MVPA studies have shown separable patterns of content decodability for current and prospective memory representations (Christophel et al., 2018; LaRocque et al., 2016, 2013; Lewis-Peacock et al., 2012; Rose et al., 2016; van Loon et al., 2018; Wolff et al., 2017; Yu and Postle, 2018), we are the first to directly decode the signals controlling the *state* of those memory representations.

3.3. Univariate time-frequency power is not sensitive to the momentary task-relevance of a single VWM representation

Next, we performed a series of more traditional univariate analyses enabling us to directly compare univariate with multivariate analysis of oscillatory EEG activity, and to make comparisons with previous research. First, posterior alpha power (8–14 Hz) was more suppressed (relative to baseline) for contralateral compared to ipsilateral electrodes, both during encoding and the first delay period (270–1420 ms relative to memory display onset, $p < 0.05$ cluster-corrected; Fig. 4a, left column). Lateralized alpha suppression during working memory encoding and maintenance is a common finding (Fukuda et al., 2015; Myers et al., 2015), and is generally interpreted as a reduction in alpha-induced "pulses" of inhibitory activity, which is thought to support the selection and processing of relevant sensory information (Jensen and Mazaheri, 2010; Klimesch et al., 2007; Zumer et al., 2014). Contrary to what we have found earlier (de Vries et al., 2018, 2017), lateralized alpha suppression during the first delay period did not dissociate between current and prospective memory representations. One explanation for this comes from the fact that the probability of having to search for the memory item in the Current condition was only 60% (as the first search display was omitted in 40% of trials), while it was 100% for the memory item in the Prospective condition. Consequently, this might have led subjects to put relatively more weight on prospective representations, which in turn cancelled out the expected effect of stronger alpha suppression for the current representation. In accordance with this explanation, a previous study that manipulated the probability with which a laterally presented memory item was tested on the first of two tasks indeed also found that alpha lateralization did not dissociate between priority states during the first delay period (van Ede et al., 2017). On the other hand, we previously did find priority-sensitivity of lateralized alpha suppression during the first delay period (de Vries et al., 2018); there, the probability manipulations were equivalent to the current study. Another possible explanation is that because on each trial only one item needed to be remembered, this eradicated the need for a spatial priority signal. However, we did previously observe lateralized alpha suppression effects of status even when only one item was remembered (de Vries et al., 2017). We suggest that the combination of the above two explanations caused the here-observed lack of a condition difference in alpha lateralization during the first delay period.

Similar to previous findings (de Vries et al., 2018; van Ede et al., 2017), lateralized alpha suppression did dissociate between priority states during the second delay period as it only reappeared for the Prospective condition (1030–1380 ms after the switch cue; $p < 0.05$ cluster corrected; Fig. 4a, right column). This was to be expected because in the second delay period of the Current condition the memory item, together with the spatial index of its location, could be dropped completely, while in the Prospective condition the priority actually shifted to the now-relevant memory item.

The above analysis focused on the hypothesized sensitivity of hemifield-specific alpha-band lateralization to the status of working memory content. Next we asked whether there could be a univariate time-frequency signature that is related to template prioritization, yet not lateralized. To answer this, we first performed an exploratory mass-univariate analysis on the condition contrast (i.e. Current versus Prospective) of alpha (8–14 Hz) power. Because we did not have a strict hypothesis about a specific time interval nor a pre-specified set of electrodes, we performed a cluster-based permutation test on alpha-band power at all time-points and all 64 electrodes. The result of this analysis did not show any pattern of alpha activity that could reliably distinguish between current and prospective memory representations, neither during the first, nor during the second delay period (Fig. 4b). Next, since frontal delta power seems involved in the control of prioritization within VWM (de Vries et al., 2018), we averaged over this a priori determined spatio-spectral ROI (i.e. 2–6 Hz, AFz/AF3) and performed the cluster test over time. However, this analysis also did not show any sensitivity to template status (data not shown). It could be that univariate oscillatory activity of different rhythmicity would be sensitive. However, applying a cluster-based permutation test on the entire time-frequency-electrode space again did not show any difference between the Current and Prospective conditions in either of the two delay periods.

Applying a cluster-based permutation test to such a large multi-dimensional space without pre-set constraints is relatively insensitive to finding true effects (Maris and Oostenveld, 2007). More importantly though, such a cluster test only assesses whether adjacent time-, frequency-, or electrode-points show an effect in the same direction and whether they form a larger cluster than expected by chance. In contrast to MVPA, this approach is therefore blind to more complex patterns of activation such as combinations of increases and decreases, or spatially more distributed patterns of activation that uniquely code for specific working memory processes. The complexity of the topographical distributions that successfully separated the status "classes" (Fig. 2c) not only explains the absence of statistical effects under the mass-univariate approach, it also shows that such univariate approaches may mask more heterogeneous underlying activity patterns.

Lastly, in our previous study we found that frontal delta power correlated with lateralized posterior alpha power during the second delay period, at the time when subjects switched priority within VWM from the first to the second search template (see Fig. 5 in de Vries et al., 2018). Furthermore, higher frontal delta power in this interval predicted a faster response in the subsequent search task. Together, these previous findings revealed a functional role of frontal delta power in switching priority between multiple representations simultaneously held in working memory. We ran equivalent correlation analyses here to investigate whether these control signals would also be present when only one template was held in memory, and thus when there was no strict *switch* between memory representations (see Supplementary Material). In short, we did not find such a correlation between frontal delta and lateralized posterior alpha power, suggesting that our previous findings are specific to *switching* priority between multiple items held in WM. More research is needed to elucidate the exact role of frontal control signals and their relation to sensory areas while preparing for sequences of perceptual tasks, perhaps using methods with higher spatial resolution such as combined MEG-fMRI (Baldauf and Desimone, 2014; Cichy et al., 2014). However, we did find a negative correlation between frontal delta power and reaction time in the subsequent search task, but only for the condition in which a template representation needed to be prepared for the upcoming task (i.e. the Current condition in the first delay period and the

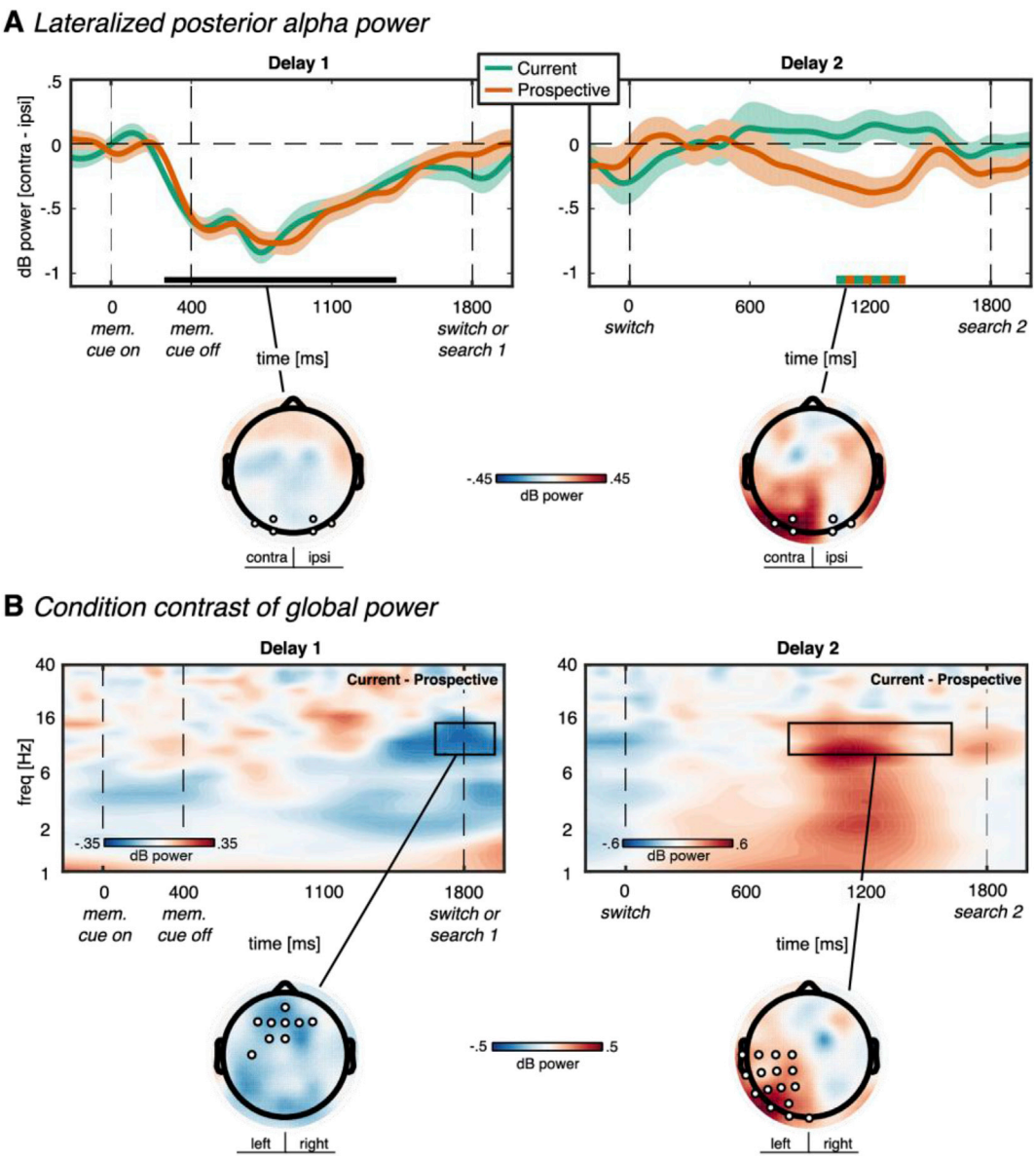

Fig. 4. Univariate time-frequency power. (a) Top: Time series of lateralized alpha (8–14 Hz) power at a priori selected electrodes (PO3/4, PO7/8, O1/2) for Current (green) and Prospective (orange) conditions. The left panel shows activity during delay 1 (all trials) and the right panel shows activity during delay 2 (only trials where first search task was omitted, i.e. 40% of all trials). Thick lines denote subject mean, shaded areas denote SEM corrected for between-subject variability (Morey, 2008). The horizontal black bar in the left panel indicates significant condition-average alpha lateralization, whereas the double-colored bar in the right panel indicates a significant condition-contrast ($p < 0.05$ cluster-corrected). Bottom: Topographies illustrate the condition-contrast of alpha power averaged over the above-mentioned two time windows. For illustrative purposes, electrode labels were flipped along the vertical midline for left-memory cue trials before averaging over trials, such that electrodes in the left and right half of the topographies are contralateral and ipsilateral to the memory cue, respectively. (b) Top: Time-frequency maps of power averaged over electrodes indicated by white disks in the topographies directly below, for the Current versus Prospective condition-contrast. Bottom: Topographies show the condition-contrast averaged over the time-frequency window indicated by the black square outline in the top time-frequency maps. As there was no significant condition-contrast after cluster-correction, the largest alpha power clusters of sub-threshold significance ($p > 0.05$) are shown for illustrative purposes. Note that statistics were done over all time-frequency-electrode points.

Prospective condition in the second delay period; Fig. S5). Note that the time interval of significant correlation largely overlaps with the time interval of above-chance delta decoding (compare Fig. 2a with Fig. S5). This directly links frontal delta power during the delay period to performance on the subsequent working memory-driven task, thus supporting our proposition that the here observed delta power decoding is specifically related to preparing for the template-based search task.

3.4. Caveats

One caveat here is that our MVPA findings do not speak to the exact nature of the neurocognitive mechanism driving the reliable classification of working memory status, other than how it manifests as band-specific patterns of EEG at the macroscopic scalp level, and that it reflects a difference in preparatory state for the upcoming task. We cannot be certain which sub-process of such preparation causes the here observed results, but we can hypothesize a number of candidates. First, the status-related signal may reflect the initialization of task priority settings (or re-initialization in the second delay) – that is, the order in which the two tasks will be done. Second, the signal may reflect the transformation of the representational state of the memory in service of the upcoming task demands (Myers et al., 2017a, b), as the memory will

be transformed into a visual search template when the template-based search task is expected. Third, the signal may be related to observers preparing for two rather different types of task, namely a template-based versus a duplicate-color search task. We argue that this latter option is less likely to be the main factor here, as the decoding differences emerged mainly early in the delay periods, rather than being closely time-locked to display onset. As such they more likely reflect preparation of the memory representation, rather than preparation for a specific task. The fact that delta power in the time window of significant classification correlated with better performance, but only in the template-based search task, further supports this interpretation. In addition, in our previous study we found oscillatory power in the same frequency bands and in a similar time window to be involved in WM prioritization, even though there all search tasks were working memory-driven (de Vries et al., 2018). However, even if the current results reflect preparation for two different tasks as such, here this still involves a distinction between a task for which a memory is required and a task for which no memory required. Nevertheless, we cannot exclude the possibility that similar signals will be involved in task-specific preparations independent of working memory requirements, and future research would benefit from designs in which these sub-processes can clearly be disentangled.

Furthermore, we would like to place a caveat with the result of the GAT analysis (Fig. 3). We can infer from this analysis that the spatial pattern of alpha power underlying above-chance decoding was stable for large parts of each delay period, whereas this was not the case for delta power (for a discussion on the interpretation of GAT see King and Dehaene, 2014). However, this does not necessarily imply that this pattern was *sustained* throughout the delay period. In fact, both in the GAT plot (Fig. 3b) and in the alpha decoding time series (Fig. 2b) gaps in significant decoding are clearly visible. However, the significant clusters in the GAT plot do indicate that whenever there was significant alpha power decoding, this was supported by the same spatial pattern of activity within that delay period (King and Dehaene, 2014), whereas this was not the case for delta power decoding (Fig. 3a). While we cannot be sure as to why alpha power decoding was not sustained throughout the delay periods, we carefully speculate that the neurocognitive process of prioritization involved two distinct intervals. That is, one during initialization of the priority cue (or re-initialization in the second delay), thereby coinciding with its control (as reflected in delta power decoding), and one later during the delay periods, likely more closely related to preparing the memory representation for the upcoming search task. As mentioned above, future research would benefit from designs in which these sub processes can clearly be disentangled.

4. Conclusions

In line with our hypothesis, we show that oscillatory signals in the delta (2–4 Hz) range play an important role in controlling the priority status of working memories between what is relevant for imminent and what is relevant for future tasks. This general result corroborates earlier evidence pointing to a key role of frontal low-frequency (delta-to-theta) oscillations in the top-down control of VWM (Johnson et al., 2017; Onton et al., 2005; Sauseng et al., 2010), task switching (Sauseng et al., 2006), and switching between two search templates (de Vries et al., 2018).

Importantly, we show such delta signals to be involved both in *implementing* priority states at the start of the task sequence, and when *switching* priority in between tasks. Interestingly, delta power decoding did not generalize over time, suggesting that control of prioritization is supported by dynamic patterns of neural activity, which moreover vary between implementing priority states and switching between such states. This complex and dynamic character fits with the operative, action-like nature of transforming the status of different representations according to their relevance (Myers et al., 2017b), and indicates that such transformations differ between initiating those states and alternating between them. In contrast, we show a more spatially stable involvement of alpha (8–14 Hz) power during both delay periods, which we consider more closely related to the maintenance of differently prioritized sensory memory representations themselves. The fact that alpha power decoding generalized within, and even across delays (as indicated by negative cross-delay decoding), indicates that at least part of the pattern underlying the maintenance of differently prioritized items is stable (cf. Stokes, 2015).

Finally, at a more methodological level, we observed that common univariate approaches did not reliably distinguish priority states of working memory representations, supporting our claim that the neural oscillatory activity underlying prioritization and the control thereof, is complex and spatially distributed, and at least partially independent of the specific location at which the memory item was initially processed. While spatial location may be used as an index when both current and prospective memories are simultaneously held in working memory (de Vries et al., 2018, 2017), we here show that it is not the only way in which these types of memory can be dissociated. Thus, our study supports the proposition that multivariate EEG approaches can be used to study more complex spatial patterns of information involved in higher order anticipatory brain states, and provides another testament to their statistical sensitivity relative to univariate approaches (LaRocque et al., 2014; Mayr and Kikumoto, 2018; Stokes et al., 2015; Van Ede et al., 2018).

Funding

This work was supported by the European Research Council (ERC) Consolidator grant (ERC-2013-CoG-615423) to CNLO. The authors declare no competing financial interests.

Author contributions

I.E.J.d.V., J.v.D., and C.N.L.O. designed the experiment; I.E.J.D.V. conducted the experiment; I.E.J.d.V. and J.v.D. analyzed the data; I.E.J.d.V., J.v.D., and C.N.L.O. wrote the paper.

Acknowledgements

We would like to thank Johannes Fahrenfort for his support with using ADAM (Amsterdam Decoding and Modeling toolbox).

Appendix A. Supplementary data

Supplementary data to this article can be found online at https://doi.org/10.1016/j.neuroimage.2019.02.069.

References

Allefeld, C., Görgen, K., Haynes, J.D., 2016. Valid population inference for information-based imaging: from the second-level t-test to prevalence inference. Neuroimage 141, 378–392. https://doi.org/10.1016/j.neuroimage.2016.07.040.

Baldauf, D., Desimone, R., 2014. Neural mechanisms of object-based attention. Science 344, 424–427. https://doi.org/10.1126/science.1247003.

Bundesen, C., 1990. A theory of visual attention. Psychol. Rev. 97, 523–547. https://doi.org/10.1037/0033-295X.97.4.523.

Carlisle, N.B., Woodman, G.F., 2011. Automatic and strategic effects in the guidance of attention by working memory representations. Acta Psychol. (Amst) 137, 217–225. https://doi.org/10.1016/j.actpsy.2010.06.012.

Christophel, T.B., Iamshchinina, P., Yan, C., Allefeld, C., Haynes, J.D., 2018. Cortical specialization for attended versus unattended working memory. Nat. Neurosci. 21, 494–496. https://doi.org/10.1038/s41593-018-0094-4.

Christophel, T.B., Klink, P.C., Spitzer, B., Roelfsema, P.R., Haynes, J.-D., 2017. The distributed nature of working memory. Trends Cognit. Sci. 21, 111–124. https://doi.org/10.1016/j.tics.2016.12.007.

Cichy, R.M., Pantazis, D., 2017. Multivariate pattern analysis of MEG and EEG: a comparison of representational structure in time and space. Neuroimage 158, 441–454. https://doi.org/10.1016/j.neuroimage.2017.07.023.

Cichy, R.M., Pantazis, D., Oliva, A., 2014. Resolving human object recognition in space and time. Nat. Neurosci. 17, 455–462. https://doi.org/10.1038/nn.3635.

Cohen, M.X., 2014. Analyzing Neural Time Series Data: Theory and Practice. MIT press.

de Vries, I.E.J., van Driel, J., Karacaoglu, M., Olivers, C.N.L., 2018. Priority switches in visual working memory are supported by frontal delta and posterior alpha

interactions. Cerebr. Cortex 28, 4090–4104. https://doi.org/10.1093/cercor/bhy223.
de Vries, I.E.J., van Driel, J., Olivers, C.N.L., 2017. Posterior alpha EEG dynamics dissociate current from future goals in working memory guided visual search. J. Neurosci. 37, 1591–1603. https://doi.org/10.1523/JNEUROSCI.2945-16.2016.
Delorme, A., Makeig, S., 2004. EEGLAB: an open source toolbox for analysis of single-trial EEG dynamics including independent component analysis. J. Neurosci. Methods 134, 9–21. https://doi.org/10.1016/j.jneumeth.2003.10.009.
Derrington, a M., Krauskopf, J., Lennie, P., 1984. Chromatic mechanisms in lateral geniculate nucleus of macaque. J. Physiol. 357, 241–265. https://doi.org/10.1113/jphysiol.1984.sp015499.
Desimone, R., Duncan, J., 1995. Neural mechanisms of selective visual attention. Annu. Rev. Neurosci. 18, 193–222.
Duncan, J., Humphreys, G.W., 1989. Visual search and stimulus similarity. Psychol. Rev. 96, 433–458. https://doi.org/10.1037/0033-295X.96.3.433.
Fahrenfort, J.J., van Driel, J., van Gaal, S., Olivers, C.N.L., 2018. From ERPs to MVPA using the Amsterdam decoding and modeling toolbox (ADAM). Front. Neurosci. 12. https://doi.org/10.3389/fnins.2018.00368.
Fukuda, K., Mance, I., Vogel, E.K., 2015. α power modulation and event-related slow wave provide dissociable correlates of visual working memory. J. Neurosci. 35, 14009–14016. https://doi.org/10.1523/JNEUROSCI.5003-14.2015.
Groppe, D.M., Makeig, S., Kutas, M., 2009. Identifying reliable independent components via split-half comparisons. Neuroimage 45, 1199–1211. https://doi.org/10.1016/j.neuroimage.2008.12.038.
Hand, D.J., Till, R.J., 2001. A simple generalisation of the area under the ROC curve for multiple class classification problems. Mach. Learn. 45, 171–186. https://doi.org/10.1023/A:1010920819831.
Haufe, S., Meinecke, F., Görgen, K., Dähne, S., Haynes, J.D., Blankertz, B., Bießmann, F., 2014. On the interpretation of weight vectors of linear models in multivariate neuroimaging. Neuroimage 87, 96–110. https://doi.org/10.1016/j.neuroimage.2013.10.067.
Helfrich, R.F., Knight, R.T., 2016. Oscillatory dynamics of prefrontal cognitive control. Trends Cognit. Sci. 20, 916–930. https://doi.org/10.1016/j.tics.2016.09.007.
Jensen, O., Mazaheri, A., 2010. Shaping functional architecture by oscillatory alpha activity: gating by inhibition. Front. Hum. Neurosci. 4, 186. https://doi.org/10.3389/fnhum.2010.00186.
Johnson, E.L., Dewar, C.D., Solbakk, A.K., Endestad, T., Meling, T.R., Knight, R.T., 2017. Bidirectional frontoparietal oscillatory systems support working memory. Curr. Biol. 27, 1829–1835 e4. https://doi.org/10.1016/j.cub.2017.05.046.
Kayser, J., Tenke, C.E., 2015. On the benefits of using surface Laplacian (current source density) methodology in electrophysiology. Int. J. Psychophysiol. 97, 171–173. https://doi.org/10.1016/j.ijpsycho.2015.06.001.
King, J.R., Dehaene, S., 2014. Characterizing the dynamics of mental representations: the temporal generalization method. Trends Cognit. Sci. 18, 203–210. https://doi.org/10.1016/j.tics.2014.01.002.
Klimesch, W., Sauseng, P., Hanslmayr, S., 2007. EEG alpha oscillations: the inhibition-timing hypothesis. Brain Res. Rev. 53, 63–88. https://doi.org/10.1016/j.brainresrev.2006.06.003.
LaRocque, J.J., Lewis-Peacock, J. a, Drysdale, A.T., Oberauer, K., Postle, B.R., 2013. Decoding attended information in short-term memory: an EEG study. J. Cogn. Neurosci. 25, 127–142. https://doi.org/10.1162/jocn_a_00305.
LaRocque, J.J., Lewis-Peacock, J. a, Postle, B.R., 2014. Multiple neural states of representation in short-term memory? It's a matter of attention. Front. Hum. Neurosci. 8, 5. https://doi.org/10.3389/fnhum.2014.00005.
LaRocque, J.J., Riggall, A.C., Emrich, S.M., Postle, B.R., 2016. Within-category decoding of information in different attentional states in short-term memory. Cerebr. Cortex 1–10. https://doi.org/10.1093/cercor/bhw283.
Lewis-Peacock, J.A., Drysdale, A.T., Oberauer, K., Postle, B.R., 2012. Neural evidence for a distinction between short-term memory and the focus of attention. J. Cogn. Neurosci. 24, 61–79. https://doi.org/10.1162/jocn_a_00140.
Lopez-Calderon, J., Luck, S.J., 2014. ERPLAB: an open-source toolbox for the analysis of event-related potentials. Front. Hum. Neurosci. 8, 1–14. https://doi.org/10.3389/fnhum.2014.00213.
Maris, E., Oostenveld, R., 2007. Nonparametric statistical testing of EEG- and MEG-data. J. Neurosci. Methods 164, 177–190. https://doi.org/10.1016/j.jneumeth.2007.03.024.
Marsman, M., Wagenmakers, E.J., 2017. Bayesian benefits with JASP. Eur. J. Dev. Psychol. 14, 545–555. https://doi.org/10.1080/17405629.2016.1259614.
Mathôt, S., Schreij, D., Theeuwes, J., 2012. OpenSesame: an open-source, graphical experiment builder for the social sciences. Behav. Res. Methods 44, 314–324. https://doi.org/10.3758/s13428-011-0168-7.
Mayr, U., Kikumoto, A., 2018. Decoding Hierarchical Control of Sequential Behavior in Oscillatory EEG Activity, 1–49. bioRxiv. https://doi.org/doi.org/10.1101/344135.
Morey, R.D., 2008. Confidence intervals from normalized data: a correction to cousineau (2005). Tutor. Quant. Methods Psychol. 4, 61–64. https://doi.org/10.3758/s13414-012-0291-2.
Myers, N.E., Chekroud, S.R., Stokes, M.G., Nobre, A.C., 2017a. Benefits of flexible prioritization in working memory can arise without costs. J. Exp. Psychol. Hum. Percept. Perform. https://doi.org/10.1037/xhp0000449.
Myers, N.E., Stokes, M.G., Nobre, A.C., 2017b. Prioritizing information during working memory: beyond sustained internal attention. Trends Cognit. Sci. 21, 449–461. https://doi.org/10.1016/j.tics.2017.03.010.
Myers, N.E., Walther, L., Wallis, G., Stokes, M.G., Nobre, A.C., 2015. Temporal dynamics of attention during encoding versus maintenance of working memory: complementary views from event-related potentials and alpha-band oscillations. J. Cogn. Neurosci. 27, 492–508. https://doi.org/10.1162/jocn.
Nobre, A.C., Van Ede, F., 2018. Anticipated moments: temporal structure in attention. Nat. Rev. Neurosci. 19, 34–48. https://doi.org/10.1038/nrn.2017.141.
Oberauer, K., Hein, L., 2012. Attention to information in working memory. Curr. Dir. Psychol. Sci. 21, 164–169. https://doi.org/10.1177/0963721412444727.
Olivers, C.N.L., Peters, J., Houtkamp, R., Roelfsema, P.R., 2011. Different states in visual working memory: when it guides attention and when it does not. Trends Cognit. Sci. 15, 327–334. https://doi.org/10.1016/j.tics.2011.05.004.
Olmos-Solis, K., van Loon, A.M., Los, S.A., Olivers, C.N.L., 2017. Oculomotor measures reveal the temporal dynamics of preparing for search. Prog. Brain Res. 236. https://doi.org/https://doi.org/10.1016/bs.pbr.2017.07.003.
Olmos-Solis, K., van Loon, A.M., Olivers, C.N.L., 2018. Pupil dilation reflects task relevance prior to search. J. Cogn. 1, 1–15. https://doi.org/10.5334/joc.12.
Onton, J., Delorme, A., Makeig, S., 2005. Frontal midline EEG dynamics during working memory. Neuroimage 27, 341–356. https://doi.org/10.1016/j.neuroimage.2005.04.014.
Oostenveld, R., Fries, P., Maris, E., Schoffelen, J.M., 2011. FieldTrip: open source software for advanced analysis of MEG, EEG, and invasive electrophysiological data. Comput. Intell. Neurosci. 2011, 156869. https://doi.org/10.1155/2011/156869.
Perrin, F., Pernier, J., Bertrand, O., Echallier, J.F., 1989. Spherical splines for scalp potential and current density mapping. Electroencephalogr. Clin. Neurophysiol. 72, 184–187. https://doi.org/10.1016/0013-4694(89)90180-6.
Peters, J.C., Goebel, R., Roelfsema, P.R., 2009. Remembered but unused: the accessory items in working memory that do not guide attention. J. Cogn. Neurosci. 21, 1081–1091.
Rerko, L., Oberauer, K., 2013. Focused, unfocused, and defocused information in working memory. J. Exp. Psychol. Learn. Mem. Cogn. 39, 1075–1096. https://doi.org/10.1037/a0031172.
Rose, N.S., LaRocque, J.J., Riggall, A.C., Gosseries, O., Starrett, M.J., Meyering, E.E., Postle, B.R., 2016. Reactivation of latent working memories with transcranial magnetic stimulation. Science 354 (80), 1136–1139.
Rouder, J.N., Speckman, P.L., Sun, D., Morey, R.D., Iverson, G., 2009. Bayesian t tests for accepting and rejecting the null hypothesis. Psychon. Bull. Rev. 16, 225–237. https://doi.org/10.3758/PBR.16.2.225.
Sauseng, P., Griesmayr, B., Freunberger, R., Klimesch, W., 2010. Control mechanisms in working memory: a possible function of EEG theta oscillations. Neurosci. Biobehav. Rev. 34, 1015–1022. https://doi.org/10.1016/j.neubiorev.2009.12.006.
Sauseng, P., Klimesch, W., Freunberger, R., Pecherstorfer, T., Hanslmayr, S., Doppelmayr, M., 2006. Relevance of EEG alpha and theta oscillations during task switching. Exp. Brain Res. 170, 295–301. https://doi.org/10.1007/s00221-005-0211-y.
Stokes, M.G., 2015. 'Activity-silent' working memory in prefrontal cortex: a dynamic coding framework. Trends Cognit. Sci. 19, 394–405. https://doi.org/10.1016/j.tics.2015.05.004.
Stokes, M.G., Wolff, M.J., Spaak, E., 2015. Decoding rich spatial information with high temporal resolution. Trends Cognit. Sci. 19, 636–638. https://doi.org/10.1016/j.tics.2015.08.016.
van Driel, J., Gunseli, E., Meeter, M., Olivers, C.N.L., 2017. Local and interregional alpha EEG dynamics dissociate between memory for search and memory for recognition. Neuroimage 149, 114–128. https://doi.org/10.1016/j.neuroimage.2017.01.031.
Van Ede, F., Chekroud, S.R., Stokes, M.G., Nobre, A.C., 2018. Decoding the influence of anticipatory states on visual perception in the presence of temporal distractors. Nat. Commun. 9. https://doi.org/10.1038/s41467-018-03960-z.
van Ede, F., Niklaus, M., Nobre, A.C., 2017. Temporal expectations guide dynamic prioritization in visual working memory through attenuated α oscillations. J. Neurosci. 37, 437–445. https://doi.org/10.1523/JNEUROSCI.2272-16.2017.
van Loon, A.M., Fahrenfort, J.J., Olivers, C.N.L., 2018. Current and Future Goals Are Represented in Opposite Patterns in Object-Selective Cortex. bioRxiv. https://doi.org/10.1101/337964.
van Loon, A.M., Olmos-Solis, K., Olivers, C.N.L., 2017. Subtle eye movement metrics reveal task-relevant representations prior to visual search. J. Vis. 17, 13. https://doi.org/10.1167/17.6.13.
Van Moorselaar, D., Olivers, C.N.L., Theeuwes, J., Lamme, V.A.F., Sligte, I.G., 2015. Forgotten but not gone: retro-cue costs and benefits in a double-cueing paradigm suggest multiple states in visual short-term memory. J. Exp. Psychol. Learn. Mem. Cogn. 41, 1755–1763. https://doi.org/10.1037/xlm0000124.
Wagenmakers, E.-J., Marsman, M., Jamil, T., Ly, A., Verhagen, J., Love, J., Selker, R., Gronau, Q.F., Šmíra, M., Epskamp, S., Matzke, D., Rouder, J.N., Morey, R.D., 2017. Bayesian inference for psychology. Part I: theoretical advantages and practical ramifications. Psychon. Bull. Rev. https://doi.org/10.3758/s13423-017-1343-3.
Wang, B., Theeuwes, J., Olivers, C.N.L., 2018. When shorter delays lead to worse memories: task disruption makes visual working memory temporarily vulnerable to test interference. J. Exp. Psychol. Learn. Mem. Cogn. 44, 722–733. https://doi.org/10.1037/xlm0000468.
Wolfe, J.M., 1994. Guided Search 2.0 A revised model of visual search. Psychon. Bull. Rev. 1, 202–238. https://doi.org/10.3758/BF03200774.
Wolff, M.J., Jochim, J., Akyurek, E.G., Stokes, M.G., 2017. Dynamic hidden states underlying working memory guided behaviour. Nat. Neurosci. 1–35. https://doi.org/10.1038/nn.4546.
Yu, Q., Postle, B.R., 2018. Different States of Priority Recruit Different Neural Codes in Visual Working Memory. bioRxiv.
Zumer, J.M., Scheeringa, R., Schoffelen, J.M., Norris, D.G., Jensen, O., 2014. Occipital alpha activity during stimulus processing gates the information flow to object-selective cortex. PLoS Biol. 12. https://doi.org/10.1371/journal.pbio.1001965.